

# Energy of the $4^{(+)}$ isomer and new bands in the odd-odd nucleus $^{74}\text{Br}$

J. Döring, J. W. Holcomb, T. D. Johnson, M. A. Riley, S. L. Tabor,  
and P. C. Womble

*Department of Physics, Florida State University, Tallahassee, Florida 32306*

G. Winter

*Forschungszentrum Rossendorf, Institut für Kern- und Hadronenphysik, O-8051 Dresden, Germany*

(Received 1 December 1992)

High-spin states of the odd-odd nucleus  $^{74}\text{Br}$  were investigated via the reactions  $^{58}\text{Ni}(^{19}\text{F}, 2pn)^{74}\text{Br}$  and  $^{65}\text{Cu}(^{12}\text{C}, 3n)^{74}\text{Br}$  at beam energies of 62 and 50 MeV, respectively. On the basis of coincidence data new levels have been introduced and partly grouped into rotational bands. Some of these new states decay to known levels of negative-parity bands built on both the ground state and the long-lived  $4^{(+)}$  isomer. Thus, an excitation energy of 13.8 keV has been deduced for the long-lived isomer in  $^{74}\text{Br}$ . The level sequences observed are interpreted in terms of Nilsson configurations in conjunction with collective excitations.

PACS number(s): 21.10.-k, 23.20.-g, 27.50.+e

## I. INTRODUCTION

In recent years there has been an increasing interest in studying the interplay between quasiparticle (qp) and collective excitations in nuclei around mass number  $A \sim 70$ –80. In these nuclei the mode of nuclear excitation depends sensitively on proton number, neutron number, angular momentum, excitation energy, and properties of the qp orbitals occupied by the unpaired particles. Most of the observed high-spin phenomena in nuclei of this mass region, such as qp alignment, band crossing, shape coexistence, core polarization, and shape driving effects, have been related to the occupation of the high- $j$  unique parity  $g_{9/2}$  subshells for protons and/or neutrons in conjunction with collective excitations.

For some neutron deficient nuclei in this mass region, for example,  $^{78}\text{Sr}$  [1],  $^{74,75}\text{Kr}$  [2–5], and  $^{75}\text{Br}$  [6–8] prolate (or near prolate) quadrupole deformations of  $\beta_2 \approx 0.31$ –0.4 have been found for the ground states and/or low-lying excited states, in agreement with cranking calculations [9]. Similar large deformations have been deduced from transition probabilities within the yrast cascades of the odd-odd nuclei  $^{74,76}\text{Br}$  [10, 11], supporting earlier particle-rotor calculations for the  $(\pi g_{9/2} \otimes \nu g_{9/2})$  configuration in  $^{76}\text{Br}$  [12]. These calculations provide a qualitative explanation for the observed signature splitting and inversion in the positive-parity cascade. Recently, a new theoretical approach [13, 14] has been developed to describe similar properties of rotational bands in doubly odd nuclei of the rare-earth region.

In the last decade several in-beam studies of the doubly odd nucleus  $^{74}\text{Br}$  have been published [10, 15–17] showing separate level schemes for the states built on top of the low-spin ground state and the high-spin isomer. On the basis of excitation function, angular distribution, and nanosecond lifetime measurements, a spin and parity of  $(0^-)$  have been proposed [16] for the ground state of  $^{74}\text{Br}$ , in agreement with experimental data from the  $^{74}\text{Kr}$  decay [18, 19].

For the high-spin isomer a spin of  $I = 4\hbar$  has been unambiguously determined in an atomic-beam magnetic-

resonance measurement [20]. The parity was originally given tentatively to be negative. Later doubts were expressed [15] about the assignment of negative parity, and positive parity was suggested [16] due to the great similarity of the band built on this isomer with a level sequence of positive parity in  $^{76}\text{Br}$ . But there is, so far, no conclusive experimental information about the energy of this  $4^{(+)}$  isomer which has a lifetime of 41.5 min [21] or 49.5 min [15]. On the basis of an excitation function measurement [22] the excitation energy was estimated to lie between the limits of 135 and 255 keV. Later it has been suggested [16] that the energy of the isomer has to be below the  $(2^-)$  level at 72.6 keV excitation energy in order to explain the absence of any decay transition from the  $4^{(+)}$  isomer to this state and to understand the long lifetime.

In the present investigation of  $^{74}\text{Br}$  two different reactions have been employed. Some results of the first one, where a 62 MeV  $^{19}\text{F}$  beam was bombarded on a highly enriched  $^{58}\text{Ni}$  target, have already been published [10]. In this publication the rotational bands proposed to feed the  $4^{(+)}$  isomer have been extended towards higher spins. In the present work the results for the medium-spin states of negative parity are mainly presented. Preliminary results have been published elsewhere [23].

## II. EXPERIMENTAL PROCEDURES AND RESULTS

Excited states in  $^{74}\text{Br}$  have been investigated by two coincidence measurements performed at the Tandem accelerator facility of the Florida State University (FSU).

In the first experiment the  $^{58}\text{Ni}(^{19}\text{F}, 2pn)^{74}\text{Br}$  reaction at 62 MeV beam energy was used. The target consisted of a 19 mg/cm<sup>2</sup> thick Ni foil enriched to 99% in  $^{58}\text{Ni}$ . The  $\gamma$  rays were detected with three Compton-suppressed high-purity (HP) Ge detectors placed at 90°, 90°, and 4° with respect to the beam axis. Prompt coincidences of more than  $6 \times 10^8$  events were stored on magnetic tape and sorted off-line after recalibration to a dispersion of 0.8 keV/channel into two arrays of (90°-90°) and (90°- 4°)

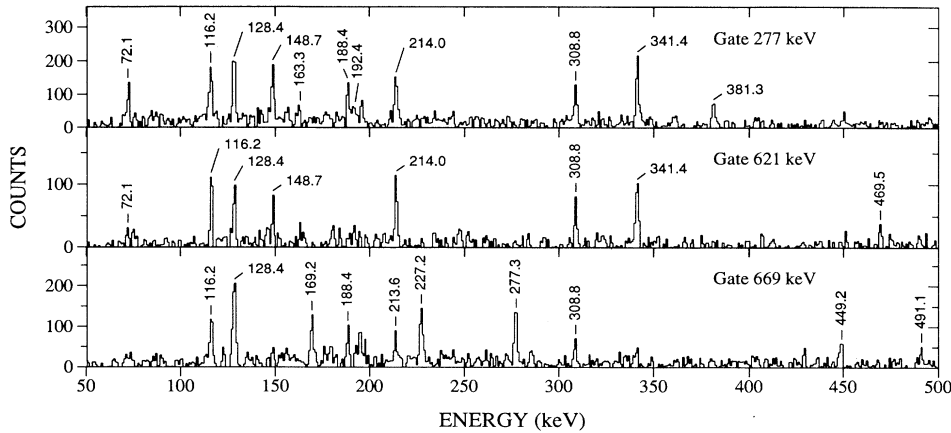


FIG. 1. Portions of background-corrected coincidence spectra obtained by gating on the  $\gamma$  rays at 277, 621, and 669 keV in the  $(90^\circ-90^\circ)$  coincidence array. These data were recorded during the bombardment of 62 MeV  $^{19}\text{F}$  ions on a  $^{58}\text{Ni}$  target.

depending on which detectors had fired.

For establishing the level scheme of  $^{74}\text{Br}$ , we analyzed  $\gamma$ -ray spectra obtained by setting gates in the  $(90^\circ-90^\circ)$  array on the peaks of interest with appropriate background subtraction. Some examples of background-corrected spectra obtained from this measurement relevant to the newly introduced levels are shown in Figs. 1 and 2. The energies and intensities of transitions assigned to  $^{74}\text{Br}$  are compiled in Table I. For some transitions, the intensities given in Table I differ from those given in Ref. [10]. The new numbers have been obtained in an independent analysis of the  $(90^\circ-90^\circ)$  coincidence data. For many transitions directional correlation of oriented nuclei (DCO) ratios were determined from coincidence gates set on  $\Delta I = 2$  transitions in the  $(90^\circ-4^\circ)$  array. In most cases the ratios given in Table I represent average values which have been deduced from individual numbers obtained from different coincidence gates, or from added coincidence spectra of relevant  $\Delta I = 2$  transitions in order to improve the statistics. Further details of the experimental setup and data handling have already been presented in Ref. [10].

A second experiment was carried out using the  $^{65}\text{Cu}(^{12}\text{C},3n)^{74}\text{Br}$  reaction at a beam energy of 50 MeV to help identify a new decay sequence. The Cu target consisted of a self-supporting foil of 0.6 mg/cm<sup>2</sup> enriched to 99% in  $^{65}\text{Cu}$ . In this experiment the Pitt-FSU detector array [24] consisting of 9 HPGe detectors with individual efficiencies between 20% and 25% has been employed. In this short experiment about  $5 \times 10^7$  prompt coincidence events were recorded on magnetic tape and sorted off-line into a total  $\gamma$ - $\gamma$  array after correction for the Doppler

shift of the  $\gamma$  rays. Threefold events were decomposed into twofold events and subsequently stored in the array which was analyzed in the same way as the matrix from the other experiment.

### III. THE LEVEL SCHEME

So far, separate level schemes have been published [10, 15–17] for the states populating the  $(0^-)$  ground state in conjunction with the  $(1^-)$  excited state at 9.8 keV and the  $4^{(+)}$  isomer in  $^{74}\text{Br}$ . In the following sections our experimental results are presented which provide evidence for linking transitions between the negative-parity level sequences built on top of the first excited state and the  $4^{(+)}$  isomer. In addition, experimental evidence is presented for a new band of negative parity feeding into the  $4^{(+)}$  isomer. Furthermore, some weakly excited states have been found decaying to the well-known level sequence of positive parity. The level scheme for  $^{74}\text{Br}$  deduced in the present work is shown in Figs. 3 and 4 for negative- and positive-parity states, respectively.

#### A. Negative-parity states

The ground state and the first excited state at 9.8 keV in  $^{74}\text{Br}$  are mainly populated by sequences containing the 89.6 keV and the 62.8 keV  $\gamma$  rays, respectively. These  $\gamma$  rays have consistently been placed in the level scheme in previous papers [15, 16]. On the basis of the  $\beta$  decay data [18, 19] in conjunction with the angular distribution and ns lifetime measurements for the  $\gamma$  rays at 89.6 and 62.8 keV spins and parities of  $(0^-)$ ,  $(1^-)$ , and  $(2^-)$  have

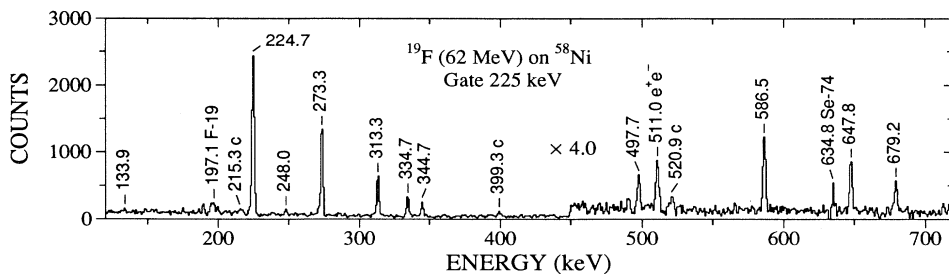


FIG. 2. Background-corrected coincidence spectrum obtained by setting a gate on the 225 keV peak measured during the irradiation of a  $^{58}\text{Ni}$  target with 62 MeV  $^{19}\text{F}$  ions. Above an energy of 450 keV the spectrum has been multiplied with a factor of 4. Peaks marked with the letter c are not assigned to  $^{74}\text{Br}$ .

TABLE I. Energies, intensities, DCO ratios, and initial state energies of  $\gamma$  rays assigned to  $^{74}\text{Br}$ .

$E_\gamma$ <sup>a</sup> (keV)	$I_\gamma$ <sup>b</sup>	$R_{\text{DCO}}$ <sup>c</sup>	$E_x$ (keV)	$E_\gamma$ <sup>a</sup> (keV)	$I_\gamma$ <sup>b</sup>	$R_{\text{DCO}}$ <sup>c</sup>	$E_x$ (keV)
62.8(1)	20(8)	-	72.6	334.7(2)	2.2(5)	0.36(14)	1384.3
72.1(1)	46(8)	-	85.9	341.4(3)	3.8(7)	0.38(9)	543.4
89.6(2)	7(2)	-	89.6	343.8(3)	$\approx 1$	-	1164.5
91.0(2)	2(1)	-	180.6	344.3(3)	2.9(6)	0.41(8)	1170.8
114.5(2)	7.5(8)	0.75(15)	485.8	344.7(3)	1.0(6)	0.55(22)	1729.0
116.2(1)	29(2)	0.42(4)	202.1	347.8(1)	27(2)	0.36(4)	1174.3
123.3(2)	1.2(5)	-	212.8	367.8(2)	2.7(6)	<0.5	1170.8
127.6(3)	2.0(6)	-	329.4	370.4(3)	3.9(6)	0.50(9)	990.1
128.2(2)	9(2)	0.61(11) <sup>d</sup>	200.8	375.8(3)	4.4(6)	1.7(3)	861.7
128.6(2)	3(1)	0.61(11) <sup>d</sup>	329.4	379.0(2)	1.6(5)	-	922.3
133.9(2)	5.0(6)	1.54(14)	619.9	381.3(2)	2.5(6)	-	1201.6
139.5(5)	1.0(4)	-	802.9	383.4(1)	19(2)	1.08(4)	397.3
140.3(2)	2.5(7)	-	212.8	392.5(3)	4.5(6)	1.17(24)	593.3
148.7(2)	2.0(5)	0.66(14)	543.4	405.8(2)	2.8(6)	0.69(14)	802.9
156.4(1)	14(1)	0.53(6)	826.5	407.8(2)	8.5(9)	0.27(4)	2068.3
159.1(2)	0.5(3)	-	339.5	411.3(2)	5.3(5)	0.26(5)	1272.9
163.3(3)	$\approx 1$	-	543.4	415.3(2)	4.9(6)	0.24(4)	1688.1
169.2(1)	23(2)	0.41(4)	371.3	417.9(2)	6.3(6)	0.95(14)	619.9
179.2(1)	5.5(7)	0.48(7)	380.0	429.2(1)	40(2)	1.07(4)	826.5
188.4(1)	19(3)	1.09(13)	202.1	430.0(4)	3(1)	-	443.7
188.5(1)	81(2)	0.24(2)	202.3	437.0(2)	2.1(6)	-	861.7
192.4(3)	0.7(5)	-	394.7	449.2(2)	2.8(6)	0.53(10)	820.7
195.0(1)	58(2)	0.25(2)	397.3	452.3(2)	2.9(6)	0.31(7)	2140.4
195.6(3)	6(1)	0.49(11)	619.9	457.7(4)	2.0(5)	0.78(21)	2441.4
213.3(2)	4.5(6)	0.53(8) <sup>d</sup>	593.3	461.1(3)	1.2(4)	-	663.4
214.0(2)	2.4(5)	0.53(8) <sup>d</sup>	543.4	467.5(2)	12(1)	1.36(25)	670.1
217.1(2)	2.2(5)	-	306.6	469.5(3)	1.3(4)	0.27(15)	1633.8
220.0(3)	1.7(5)	-	663.4	475.9(3)	3.8(5)	0.20(9)	2616.3
222.4(2)	10(1)	0.43(12)	424.5	485.9(3)	2.2(4)	-	815.6
222.4(2)	2(1)	-	815.6	486.3(2)	1.7(4)	0.15(4)	1660.5
224.4(2)	5(1)	0.68(7) <sup>d</sup>	463.1	490.4(2)	6(1)	1.29(10)	861.7
224.9(2)	7(1)	0.68(7) <sup>d</sup>	238.7	491.1(2)	3(1)	1.4(3)	820.7
227.2(2)	2.1(7)	0.47(9)	820.7	497.6(3)	2.0(5)	0.69(28)	1983.6
233.9(3)	2(1)	-	306.6	497.7(2)	2.3(5)	-	736.4
241.4(2)	4.2(5)	-	443.7	504.1(3)	3(1)	1.4(4)	1174.3
241.8(2)	5.3(6)	0.47(5)	861.7	504.3(3)	6.8(7)	0.48(6)	990.1
242.0(2)	1.3(4)	-	1164.5	511.0(4)	$\approx 1$	-	2000.1
243.8(4)	1.7(7)	-	329.4	527.6(2)	8.7(9)	0.18(7)	1197.6
248.0(3)	<0.6	-	485.8	542.3(3)	4.0(6)	1.19(22)	922.3
248.6(2)	4.3(6)	0.25(4)	619.9	586.5(3)	2.5(6)	1.04(24)	1049.7
256.6(3)	0.9(6)	-	329.4	600.4(3)	4.8(7)	0.40(18)	802.9
259.9(5)	$\approx 1$	-	1892.9	608.3(3)	3.9(6)	-	1201.6
263.8(3)	2.1(5)	0.49(12)	593.3	613.1(3)	3(1)	-	2506.1
266.1(3)	1.4(5)	0.53(15)	663.4	618.8(3)	4.2(6)	1.28(23)	990.1
272.2(3)	2.4(5)	-	815.6	621.1(3)	3.5(6)	-	1164.5
272.8(1)	26(2)	0.29(3)	670.1	647.8(3)	2.4(5)	-	1384.3
273.3(2)	4(1)	0.44(16)	736.4	653.0(2)	8.4(6)	1.06(8)	1272.9
277.3(2)	2.4(6)	0.54(22)	820.7	668.6(3)	4.2(6)	0.80(16)	1489.3
283.0(3)	2(1)	1.18(14) <sup>d</sup>	1272.9	678.7(3)	2.2(4)	0.50(12)	1164.5
283.8(2)	17(1)	1.18(14) <sup>d</sup>	485.8	679.2(3)	1.8(5)	-	1729.0
285.5(2)	12(1)	1.03(13)	371.3	682.7(3)	1.9(5)	-	1486.0
287.3(3)	2.3(4)	-	1489.3	697.9(3)	1.6(6)	<0.5	2766.0
290.8(3)	1.8(5)	<0.4	1488.3	698.0(3)	2.0(6)	1.07(12)	1688.1
307.6(2)	2.0(5)	0.73(35)	380.0	711.5(3)	2.0(5)	1.3(4)	1633.8
308.8(2)	3.3(5)	0.32(7)	394.7	728.5(3)	3(2)	0.80(21)	1892.9
311.6(3)	1.6(4)	0.44(8)	1486.0	786.8(3)	5.6(7)	1.02(9)	1272.9
313.3(2)	3.0(5)	0.49(15)	1049.7	798.5(3)	3.6(6)	0.96(17)	2000.1
315.2(3)	3.0(5)	0.51(8)	1486.0	800.1(2)	6.1(6)	0.99(14)	1197.6
322.7(4)	0.7(3)	0.54(12)	1983.6	815.6(3)	2.2(4)	-	1486.0
331.7(4)	$\approx 1$	-	2331.6	818.2(2)	6.5(8)	1.07(10)	1488.3

TABLE I. (Continued).

$E_\gamma$ <sup>a</sup> (keV)	$I_\gamma$ <sup>b</sup>	$R_{\text{DCO}}$ <sup>c</sup>	$E_x$ (keV)	$E_\gamma$ <sup>a</sup> (keV)	$I_\gamma$ <sup>b</sup>	$R_{\text{DCO}}$ <sup>c</sup>	$E_x$ (keV)
826.4(2)	7.7(7)	0.86(10)	1688.1	1089.1(3)	5.8(7)	0.11(3)	2263.4
833.9(2)	23(2)	0.94(5)	1660.5	1105.7(4)	7(1)	1.09(6) <sup>d</sup>	2766.0
842.3(3)	3(1)	1.05(13)	2331.6	1108.6(5)	13(2)	1.09(6) <sup>d</sup>	3176.9
867.4(2)	11(1)	0.99(8)	2140.4	1173.8(5)	3(1)	-	3308.2
872.3(4)	2.0(7)	-	2506.1	1184.9(5)	4(1)	-	4341.2
894.1(2)	10(1)	0.90(7)	2068.3	1224.4(5)	5(1)	-	4908.8
903.0(3)	3.1(6)	0.85(14)	1892.9	1240.2(5)	2(1)	<0.5	3308.2
928.2(2)	7.8(7)	0.84(8)	2616.3	1315.5(5)	6.2(8)	-	4492.4
936.7(3)	0.9(4)	-	2134.1	1331.2(5)	5.0(8)	-	4097.2
940.4(4)	3.1(5)	1.06(31)	2833.3	1378.5(5)	2(1)	<0.5	3446.8
955.4(3)	2.1(5)	-	2441.4	1470.0(5)	2(1)	-	5962.4
959.8(3)	5.6(7)	0.13(3)	2134.1	1517.4(5)	2(1)	-	5614.6
1015.9(4)	10(1)	1.02(15)	3156.3	1652.2(5)	2(1)	-	7614.6
1068.1(3)	6.7(8)	1.09(15)	3684.4				

<sup>a</sup>Errors in the last digit are shown in parentheses.

<sup>b</sup>Intensities deduced from the (90°-90°) array of the  $^{58}\text{Ni}(^{19}\text{F}, 2pn)^{74}\text{Br}$  measurement.

<sup>c</sup>DCO ratios are average values deduced from the  $^{58}\text{Ni}(^{19}\text{F}, 2pn)^{74}\text{Br}$  measurement.

<sup>d</sup>Effective composite value for unresolved lines.

been proposed [16] for the ground state, the first excited state at 9.8 keV, and the second excited state at 72.6 keV, respectively.

The known level sequences of negative parity built on the ground state and the first excited state have been observed in the present coincidence experiments, as shown in our level scheme (see Fig. 3). Thus, the levels on top of these two states published in Ref. [16] could be confirmed. In agreement with that paper we also do not see a coincidence between the  $\gamma$  rays at 128.2 and 307.6 keV as proposed in Ref. [15]. In addition, the sequence containing the 62.8 keV  $\gamma$  ray could be extended up to a state at 2506.1 keV with probable spin and parity of  $(10^-)$ . It has been found that the lower-lying  $\Delta I = 1$  transitions of the 62.8 keV sequence show clear coincidences with a 227.2 keV  $\gamma$  ray. Therefore, a new level at 820.7 keV has been introduced. Furthermore, coincidence pairs of 214.0-277.3 and 128.6-277.3 keV have been found but not the pair of 392.5-277.3 keV. Moreover, the  $\gamma$ -ray peak at 214 keV has been identified to be a doublet. On this basis a new level has been established at 543.4 keV excitation energy. It should be mentioned that a coincidence pair 213.4-277.0 keV has been reported previously [15] but placed on another position in the low-spin level scheme. In our coincidence spectra gated by the 277.3 keV  $\gamma$  ray in addition to the low-lying  $\gamma$  rays of the 62.8 keV sequence (e.g., the composite  $\gamma$ -ray peak at 128.4 keV) the 72.1 keV  $\gamma$  ray and several  $\gamma$  rays of the sequence built on top of the 85.9 keV level (116.2 keV sequence) have been observed. But there is less agreement in the published papers regarding the placement of this 72.1 keV transition in the level scheme. In Ref. [15] this  $\gamma$  ray is placed on top of a low-spin  $(0, 1^-)$  state at low energy ( $E_x < 30$  keV) which has no connection to any other known state of  $^{74}\text{Br}$ . In Ref. [17] it is placed on the ground state and in Ref. [16] it is proposed that the 72.1 keV  $\gamma$  ray and the 116.2 keV sequence feed into the  $4^{(+)}$  isomer. The latter placement is confirmed in a more recent paper [10]

due to the strong population of this band in heavy-ion reactions.

The puzzle of the placement of the 116.2 keV sequence has now been solved on the basis of our coincidence data as shown in the level scheme given in Fig. 3. The newly introduced levels at 543.4 and 820.7 keV decay also, e.g., via  $\gamma$  rays at 341.4 and 449.2 keV, respectively, to members of the 116.2 keV  $\gamma$ -ray sequence. The depopulation of these levels can be seen in the background-corrected coincidence spectra gated by the feeding transitions at 621.1 and 668.6 keV (see Fig. 1). In these coincidence spectra we observed low-lying transitions assigned earlier to both the 62.8 and the 116.2 keV level sequences. There are also some linking transitions, e.g., at energies of 148.7, 678.7, and 903.0 keV which connect the new level sequence built on the 329.4 keV level to known side-feeding states of the 116.2 keV sequence.

Consequently, from the new decay scheme an excitation energy of 13.8 keV has been determined for the level fed by the 72.1 keV transition. If we adopt the conclusion [10, 16] that this level corresponds to the  $4^{(+)}$  isomer, a very low excitation energy is obtained and, thus, the excitation energies of all states feeding into this isomer are fixed for the first time.

Moreover, it has been found that the levels at 329.5 and 315.9 keV given in Ref. [16] independently from each other match energetically to the same level at 329.4 keV if the energy of the isomer is taken into account, as verified from our coincidence data. A  $(3^-)$  assignment for the level at 315.9 keV is given in Fig. 5b of Ref. [16] although the angular distribution coefficients for the de-exciting  $\gamma$  rays at 127.6 and 243.8 keV shown in Table 1 of that paper would be more compatible with a  $(4^-)$  assignment, as proposed for the level at 329.5 keV in Fig. 5a of Ref. [16].

Obviously, this  $(4^-)$  state is fed by a sequence of  $\Delta I = 2$  transitions at 491.1, 668.6, and 842.3 keV which exhibit rotational band properties. Also the  $(5^-)$  state

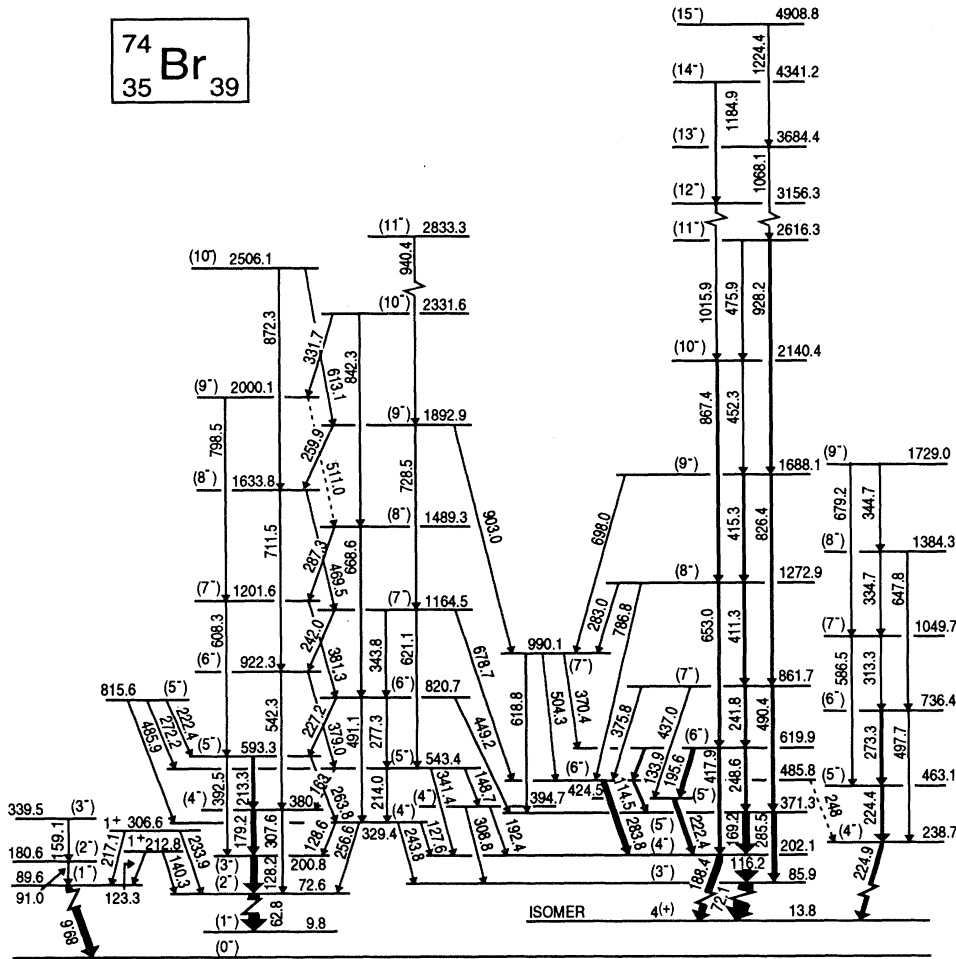


FIG. 3. Level scheme of negative-parity states built on the ground state, the first excited state at 9.8 keV, and the  $4^{(+)}$  isomer in  $^{74}\text{Br}$ . The thickness of the arrow indicates the transition intensity. Note the two changes in scale at 20 and 2500 keV excitation energy.

at 543.4 keV shows a similar feeding pattern. Therefore, we suppose that the level at 329.4 keV forms a bandhead for a new collective structure of negative parity.

Spin assignments to the new levels are partly based on DCO ratios. They support our spin assignments of  $I = (5)\hbar$  and  $(6)\hbar$  to the levels at 543.4 and 820.7 keV, respectively. Negative parity of these states is suggested by the observed decay pattern, e.g., the 820.7 keV level decays via  $\Delta I = 1, 2$  transitions to known states of negative parity. It is interesting to note that the level at 543.4 keV decays via  $\Delta I = 1$  transitions only. A decay branch to the  $(3^-)$  level at 85.9 keV has not been observed.

The sequence built on the 85.9 keV level has been observed recently [10] up to a  $(15^-)$  state at  $4895.0 + X$  keV. In addition, we do see the side-feeding transitions at energies of 114.5, 133.9, 195.6, 222.4, 283.8, 308.8, 504.3, and 786.8 keV reported previously [16, 17] and can confirm their placement in the level scheme (see Fig. 3). In addition, some new interband transitions, e.g., at energies of 370.4, 437.0, 618.8, and 698.0 keV between some of these states and the 116.2 keV sequence, have been identified. These transitions raise the confidence level for the given tentative spin and parity assignments. Only the transitions which have been introduced [17] on top of the  $977.0 + X$  keV level which is mainly depopulated by a 504.3 keV  $\gamma$  ray cannot be confirmed from our coinci-

dence data.

In the neighboring nucleus  $^{76}\text{Br}$  [25] some negative-parity states decay also to the lowest excited states of the positive-parity cascade. A search for such linking transitions in  $^{74}\text{Br}$  has been attempted but no such transitions have been observed.

#### B. A new decay sequence built on a 238.7 keV level

A new level sequence has been found and assigned to  $^{74}\text{Br}$  as shown in Fig. 3. The lowest transition with an energy of 224.9 keV shows coincidences with a  $\gamma$  ray at nearly the same energy and with several more transitions. Also  $\Delta I = 2$  in-band transitions have been observed but they are weaker in intensity compared to the  $\Delta I = 1$  transitions. A relevant coincidence spectrum obtained from the  $(90^\circ-90^\circ)$  matrix of the  $^{58}\text{Ni}(^{19}\text{F}, 2pn)^{74}\text{Br}$  reaction is presented in Fig. 2.

The assignment of this band to  $^{74}\text{Br}$  is based on the following facts.

(i) The 224.9 keV transition and the sequence on top of it (224.4 keV sequence) has been observed in the data set where a  $^{58}\text{Ni}$  target was bombarded with 62 MeV  $^{19}\text{F}$  ions. During this irradiation, evaporation reactions take place leading to final nuclei of Kr, Br, Se, or As. The  $\gamma$  rays originating from most of these nuclei

could be identified, but the new transitions did not show any prompt coincidence relationship to known  $\gamma$  rays of any identified nucleus. From the total projection of this  $\gamma$ - $\gamma$  coincidence array an intensity ratio of  $I_\gamma(\text{SUM } 224 \text{ keV})/I_\gamma(\text{SUM } 188 \text{ keV}) = 10.7(9)\%$  has been deduced. This number points to a medium-strong reaction channel. Thus, an assignment to the odd-odd nucleus  $^{74}\text{Br}$  is more probable than to Kr, Se, or As isotopes.

In order to narrow our suggestion an additional experiment has been performed where the Kr isotopes cannot be produced. For this purpose a  $^{65}\text{Cu}$  target has been bombarded with 50 MeV  $^{12}\text{C}$  ions. The compound nucleus formed by this target-projectile combination is  $^{77}\text{Br}$  and the production of Kr isotopes is excluded. But still, the sequence of interest was also observed. From the total projection of this measurement an intensity ratio  $I_\gamma(\text{SUM } 224 \text{ keV})/I_\gamma(\text{SUM } 188 \text{ keV}) = 10.2(5)\%$  has been determined which is very close to the number found in the  $^{58}\text{Ni}(^{19}\text{F}, 2pn)^{74}\text{Br}$  reaction.

A possible assignment to Se or As isotopes may not be ruled out from these experiments. Therefore, the coincidence data from an experiment has been checked where a natural Ga target was irradiated with  $^7\text{Li}$  ions of 35 MeV energy. In this experiment compound nuclei of  $^{76,78}\text{Se}$  were produced excluding the chain of Br isotopes in the set of final nuclei. Here the  $\gamma$  rays were also measured

with the Pitt-FSU array, mainly to investigate the high-spin behavior of some light As and Se isotopes [26]. But in this measurement the sequence of interest could not be observed. Thus, as a result of these cross reaction measurements an assignment to  $^{74}\text{Br}$  is strongly suggested.

(ii) Gamma rays at energies of 224.2(2) and 225.0(2) keV have also been observed [16] via  $^3\text{He}$  and deuteron induced reactions on a  $^{74}\text{Se}$  target and have been assigned to  $^{74}\text{Br}$  as shown in Table 1 of that paper. However, these  $\gamma$  rays were not placed in the level scheme.

(iii) A search for linking transitions to the other known states of  $^{74}\text{Br}$  has been done but no firm connection could be found. There are some weak peaks, e.g., peaks at 133.9 and 248.0 keV in the 225 keV gate and some more in various coincidence spectra which would support the present placement in the level scheme. But these transitions are in most cases members of complex line groups and the weak peaks may also be interpreted as arising from other reaction channels.

On the basis of our intensities and the published [16] excitation functions for the 224.2 and 225.0 keV lines we suggest that this sequence populates the  $4^{(+)}$  isomer. Moreover, a spin of  $4\hbar$  is proposed for the level at 238.7 keV excitation energy which would be in agreement with the angular distribution data given in that paper. Negative parity is suggested from systematic considerations.

### C. Positive-parity states

In the former investigations [15–17] a decay sequence containing intense  $\gamma$  rays at 188.5, 195.0, 272.8 keV, etc. has been placed unambiguously on top of the  $4^{(+)}$  isomer due to its strong population in  $^3\text{He}$  or heavy ion induced reactions. Very recently, the placement of this sequence was confirmed and the band was extended [10] up to a state with spin and parity of  $(19^+)$  at  $7600.9 + X$  keV. Additional side-feeding states decaying to members of this sequence have been observed earlier, too. These known states deexcite via  $\gamma$  rays at 241.4, 527.6, 600.4, 800.1, 818.2, 959.8, and 1089.1 keV. From the present coincidence data the placement of these side-feeding transitions in the level scheme could be confirmed and some new transitions have been found. They are shown together with the main sequence in Fig. 4. The new levels at energies of 1170.8, 1486.0, 1983.6, and 2441.4 keV seem to form a rotational-like band built on the  $(6^+)$  level at 802.9 keV.

### IV. DISCUSSION

The decay scheme of the excited states in  $^{74}\text{Br}$  as found in the present investigation exhibits a large number of states at medium spin and many decay branches in between. This observation reflects the large variety of states as expected from the occupation of the  $p_{1/2}$ ,  $p_{3/2}$ ,  $f_{5/2}$ , or the high- $j$  intruder  $g_{9/2}$  subshells by the unpaired particles and their interplay with collective excitations. Based on the large deformation deduced for  $^{74}\text{Br}$  we will attempt to discuss the observed structures as excitations of an axially deformed nucleus. Moreover, a comparison of low-lying proton states in  $^{73}\text{Br}$  [27] and  $^{75}\text{Br}$  [6–8] gives evidence for the presence of nonaxial deformations in the light Br isotopes. Therefore, some of the 2-qp states ob-

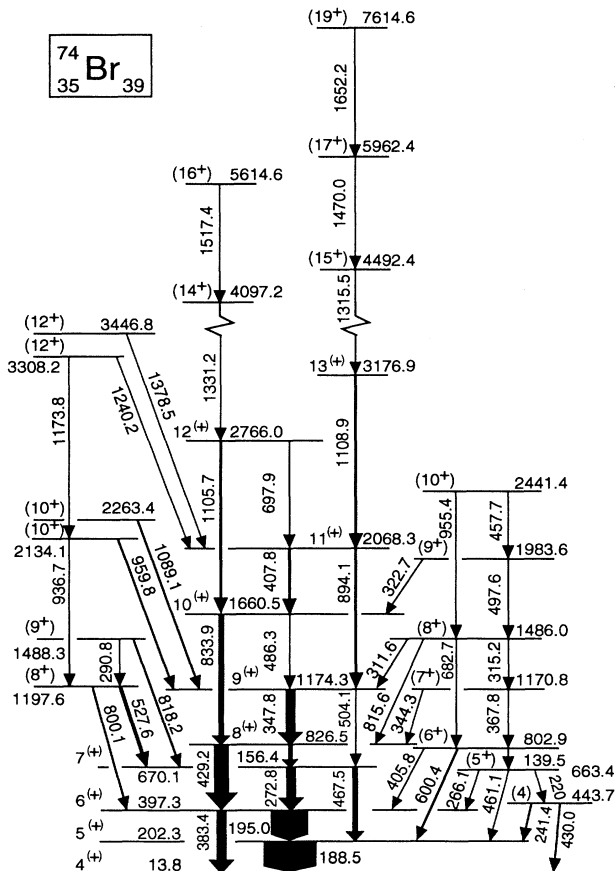


FIG. 4. Level scheme of positive-parity states feeding into the  $4^{(+)}$  isomer of  $^{74}\text{Br}$ . Above an excitation energy of 3500 keV the scale has been compressed by a factor of 2.

served in  $^{74}\text{Br}$  might be connected with nonaxial or even oblate deformation.

### A. Nilsson orbitals

The single-particle orbitals that are relevant for the movements of both the unpaired proton and neutron were calculated [9] using the Woods-Saxon potential and are shown in Fig. 1 of that paper. Calculations of the equilibrium shape predict large prolate (or near prolate) deformations of  $\beta_2 \geq 0.30$  for states in odd-mass nuclei with  $N \leq 42$ , which have experimentally been found, e.g., in  $^{75,77}\text{Kr}$  [5, 28, 29] and  $^{75}\text{Br}$  [6–8]. For prolate deformation of this size the following Nilsson configurations  $[310]_{\frac{1}{2}}^{-}$ ,  $[312]_{\frac{3}{2}}^{-}$ ,  $[440]_{\frac{1}{2}}^{+}$ , and  $[431]_{\frac{3}{2}}^{+}$  are considered for protons, and  $[422]_{\frac{5}{2}}^{+}$  and  $[301]_{\frac{3}{2}}^{-}$  for neutrons. At smaller deformation there are additional Nilsson orbitals, the  $[301]_{\frac{3}{2}}^{-}$  for protons and the  $[303]_{\frac{5}{2}}^{-}$  for neutrons. In the following we shall employ these single-particle states to discuss the observed 2-qp states in the odd-odd nucleus  $^{74}\text{Br}$ . The proposed 2-qp Nilsson configurations should be considered as the dominating structure besides some other contributions which may arise from configuration mixing of states with  $\Delta K = 1$  due to the Coriolis force or of states with  $\Delta K = 0$  due to the proton-neutron residual interaction.

### B. Excitation energy of the $4^{(+)}$ isomer

The excitation energy of 13.8 keV found for the  $4^{(+)}$  isomer of  $^{74}\text{Br}$  is in accordance with the latest prediction [16], but much lower than expected from the excitation function measurement [22]. It fits the systematics of the heavier doubly odd Br nuclei as shown in Fig. 5. In this figure the excitation energies of the isomeric states and the  $2^{-}$  states are plotted relative to the ground state of each nucleus. The  $(1^{-})$  state in  $^{74}\text{Br}$ , which has been observed at an energy of 9.8 keV above the ground state, very probably corresponds to the  $1^{-}$  ground state of  $^{76}\text{Br}$  (see Sec. IV E). The low excitation energy of the  $4^{(+)}$  isomer in  $^{74}\text{Br}$  gives a natural explanation for the long

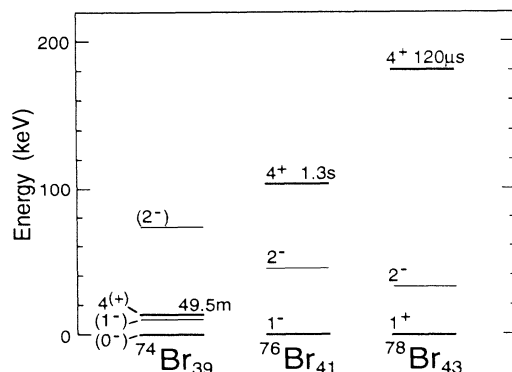


FIG. 5. Comparison of the excitation energies of the long-lived  $4^{(+)}$  isomers in  $^{74,76,78}\text{Br}$  relative to the ground states. The experimental data has been taken for  $^{76}\text{Br}$  from Refs. [30, 31] and for  $^{78}\text{Br}$  from Ref. [32].

lifetime. A decay to the  $2^{-}$  level by an  $M2$  transition as observed in the heavier isotopes is excluded and, thus, a  $\beta$  decay to  $^{74}\text{Se}$  is more likely than a decay via a 4.0 keV  $E3$  transition to the  $(1^{-})$  state or via a 13.8 keV  $M4$  transition to the  $(0^{-})$  ground state.

The  $4^{(+)}$  isomer and the high-spin level sequence of positive parity built on it have been discussed previously in terms of the 2-qp configuration  $(\pi g_{9/2} \otimes \nu g_{9/2})$  and collective excitations. This assignment has been suggested in Ref. [15] on the basis of similarities with bands in  $^{76}\text{Br}$  and  $^{78}\text{Br}$  and in Ref. [16] due to the irregularities in the level spacings for the states between  $4^{(+)}$  and  $8^{(+)}$  which have been attributed to the influence of 2-qp components. Further evidence supporting this interpretation has been obtained from the experimental signature splitting of the high-spin band of positive parity on top of this isomer [10].

The low excitation energy of the isomer points to a strongly deformed shape which has already been deduced from transition probabilities for the  $\gamma$  rays in the positive-parity sequence, e.g., an axial deformation of  $\beta_2 = 0.38$  [10] has been determined from the  $6^{(+)} \rightarrow 4^{(+)}$  transition probability in  $^{74}\text{Br}$ . For a prolate deformation of this size the low- $\Omega$  single particle orbitals of the  $g_{9/2}$  subshell are sufficiently lowered in energy that they can be occupied by the unpaired proton and neutron at very low excitation energy.

### C. Magnetic moment of the $4^{(+)}$ isomer

Recently, for the  $4^{(+)}$  isomer the magnetic moment has been measured [33] to be  $\mu = \pm 1.63(6)\mu_N$  which gives a  $g$  factor of  $g = \pm 0.41(2)$ . In their discussion in terms of Nilsson configurations only negative parity of the isomer was considered. But the experimental value of the magnetic moment does, however, not contradict with an interpretation in terms of configurations arising from the  $\pi g_{9/2}$  and  $\nu g_{9/2}$  orbitals and forming a state with  $I^\pi = 4^+$ .

If we adopt the positive sign of the deduced  $g$  factor then its value can be well reproduced using the additivity rule for the 2-qp configuration  $(\pi g_{9/2} \otimes \nu g_{9/2})$  which is in this case independent on the spins of the states. A number of  $g_{\text{cal}} = +0.466(3)$  can be calculated using the single particle  $g$  factors [34] for  $g_{9/2}$  protons taken from the  $\frac{9}{2}^+$  state in  $^{73}\text{As}$ ,  $g = 1.163(3)$ , and for  $g_{9/2}$  neutrons taken from the  $\frac{9}{2}^+$  state in  $^{71}\text{Ge}$ ,  $g = -0.231(1)$ . A similar interpretation has recently been proposed for a  $6^+$  isomer in  $^{80}\text{Rb}$  [35], where the experimental  $g$  factor,  $g_{\text{exp}} = +0.56(1)$ , can be well understood as arising from the 2-qp configuration  $(\pi g_{9/2} \otimes \nu g_{9/2})$ .

Moreover, the assumed positive value of the magnetic moment can also be reproduced by calculations in the Nilsson model employing configurations of the  $g_{9/2}$  subshells for both protons and neutrons. Numbers of  $\mu = +1.35\mu_N$  and  $+2.5\mu_N$  have been obtained for the 2-qp Nilsson configurations  $(\pi[431]_{\frac{3}{2}}^{+} \otimes \nu[422]_{\frac{5}{2}}^{+})4^+$  and  $(\pi[422]_{\frac{5}{2}}^{+} \otimes \nu[431]_{\frac{3}{2}}^{+})4^+$ , respectively, at a prolate deformation of  $\beta_2 = 0.27$ . These calculations have been performed using values of  $\kappa^\pi = 0.0695$ ,  $\mu^\pi = 0.425$ ,  $g_1^\pi$

$= 1.0$ , and  $g_s^{\pi, \text{free}} = +5.58$  for protons as well as  $\kappa^\nu = 0.0730$ ,  $\mu^\nu = 0.320$ ,  $g_l^\nu = 0.0$ , and  $g_s^{\nu, \text{free}} = -3.82$  for neutrons. An attenuation of  $g_s^{\text{eff}} = 0.6g_s^{\text{free}}$  has been used for both protons and neutrons. The collective part of the  $g$  factor has been approximated by  $g_R = Z/A$ .

Configuration mixing with  $K = 3$  and  $5$  states was not included in the calculations, although we are aware that at deformations  $\beta_2 < 0.3$  the proton orbital  $[440]_{\frac{1}{2}}^+$  may strongly contribute to the wave function of the  $4^{(+)}$  isomer. Since no mixing calculation has been performed, it is not clear how much these components would affect the magnetic moment. However, the calculations performed can already reproduce the size of the magnetic moment well.

Thus, we suggest the Nilsson configurations  $(\pi[431]_{\frac{3}{2}}^+ \otimes \nu[422]_{\frac{5}{2}}^+)4^+$  as the dominating structure forming the  $4^{(+)}$  isomer, where the particle angular momentum components are coupled parallel to each other,  $K = \Omega_p + \Omega_n$ . The same Nilsson configurations but with antiparallel coupling of the particle angular momentum components,  $K = |\Omega_p - \Omega_n|$ , have previously been suggested for the  $1^+$  state at an excitation energy of 306.6 keV [16]. The energy separation between both intrinsic states is 292.8 keV. The low-lying intrinsic state with parallel coupling mode is in agreement with predictions by the Gallagher and Moszkowski coupling rule (GM rule) [36].

It should be mentioned that the previously proposed 2-qp configuration [20, 33] with the assumption of negative parity for the isomer  $(\pi[301]_{\frac{3}{2}}^- \otimes \nu[422]_{\frac{5}{2}}^+)4^-$  gives a calculated magnetic moment of  $\mu = +1.71\mu_N$ . But the occupation of the odd parity  $[301]_{\frac{3}{2}}^-$  Nilsson orbital by the unpaired proton is very unlikely at low excitation energy and a prolate deformation of  $\beta_2 \approx 0.37$ .

A compilation of the most probable Nilsson configurations assigned to states in  $^{74}\text{Br}$  is given in Table II.

#### D. $K^\pi = (0^-)$ ground state

The  $(0^-)$  ground state of  $^{74}\text{Br}$  has been interpreted [16] as arising from the 2-qp Nilsson configuration  $(\pi[431]_{\frac{3}{2}}^+ \otimes \nu[301]_{\frac{3}{2}}^-)0^-$ . The employment of the neutron orbital

$[301]_{\frac{3}{2}}^-$  is supported by the observation of rotational bands built on low-lying  $\frac{3}{2}^-$  isomeric states in the neighboring odd-neutron nuclei  $^{73}\text{Se}$  [37] and  $^{75,77}\text{Kr}$  [5, 28, 29]. The proton orbital  $[431]_{\frac{3}{2}}^+$  had to be used in order to get  $K^\pi = 0^-$  and is now justified through its inclusion in the configuration of the low-lying  $4^{(+)}$  isomer. However, the configuration proposed for the  $0^-$  state contradicts with the prediction of the GM rule. A possible explanation might be the odd-even shift for  $K = 0$  bands due to the residual interaction between the odd proton and odd neutron [38] as discussed in the well deformed odd-odd nucleus  $^{166}\text{Ho}$  [39]. Unfortunately, the corresponding  $K^\pi = 3^-$  intrinsic state is not known in  $^{74}\text{Br}$ .

Another 2-qp configuration for the  $(0^-)$  ground state in accordance with the GM rule would be  $(\pi[303]_{\frac{5}{2}}^- \otimes \nu[422]_{\frac{5}{2}}^+)0^-$ . However, for the occupation of the  $[303]_{\frac{5}{2}}^-$  Nilsson orbital by the unpaired proton a smaller deformation ( $\beta_2 < 0.2$ ) has to be assumed which is less probable.

#### E. $K^\pi = (1^-)$ band built on the 9.8 keV level

The  $(1^-)$  state at 9.8 keV in  $^{74}\text{Br}$  is well known from decay studies [18, 19] and in-beam investigations [15, 16]. Thus, the 2-qp Nilsson configurations  $(\pi[312]_{\frac{3}{2}}^- \otimes \nu[422]_{\frac{5}{2}}^+)1^-$  have been proposed where the energetical favored state is obtained by antiparallel coupling of the particle angular momentum components. In the adjacent nucleus  $^{76}\text{Br}$  the  $1^-$  state forms the ground state and the measured magnetic moment can be well interpreted [20] in terms of these 2-qp Nilsson configurations. The rotational bands observed in  $^{74,76}\text{Br}$  on top of this state support the assumption that it is a bandhead.

The band built on the  $(1^-)$  state at 9.8 keV in  $^{74}\text{Br}$  has been extended up to a  $(10^-)$  level. The  $(2^-)$  state at 72.6 keV involved in this band deexcites via a strong  $M1$  transition [ $B(M1) > 0.13$  Weisskopf units, Ref. [16]] to the  $(1^-)$  state suggesting that both states belong to the same band. Also, the  $(3^-)$  state at 200.8 keV is considered to be a band member, even though the  $E2$  transition to the  $(1^-)$  state at 9.8 keV has not been observed. The moment-of-inertia parameters  $\hbar^2/(2\Theta)$  are given in

TABLE II. Energies, spins, and Nilsson configurations proposed for bandhead states in  $^{74}\text{Br}$ .

$E_x$ (keV)	$I^\pi$	Proton ( $\pi$ )	Neutron ( $\nu$ )	Coupling <sup>a</sup>	Ref.
0.0	$(0^-)$	$[431]_{\frac{3}{2}}^+$	$[301]_{\frac{3}{2}}^-$	$\uparrow \downarrow$	[16]
9.8	$(1^-)$	$[312]_{\frac{3}{2}}^-$	$[422]_{\frac{5}{2}}^+$	$\uparrow \downarrow$	[16, 20]
329.4	$(4^-)$	$[312]_{\frac{3}{2}}^-$	$[422]_{\frac{5}{2}}^+$	$\uparrow \uparrow$	this work
13.8	$4^{(+)}$	$[431]_{\frac{3}{2}}^+$	$[422]_{\frac{5}{2}}^+$	$\uparrow \uparrow$	this work
306.6	$1^+$	$[431]_{\frac{3}{2}}^+$	$[422]_{\frac{5}{2}}^+$	$\uparrow \downarrow$	[16]
89.6	$(1^-)$	$[431]_{\frac{3}{2}}^+$	$[303]_{\frac{5}{2}}^-$	$\uparrow \downarrow$	[16]
238.7	$(4^-)$	$[431]_{\frac{3}{2}}^+$	$[303]_{\frac{5}{2}}^-$	$\uparrow \uparrow$	this work
85.9	$(3^-)$	$[310]_{\frac{1}{2}}^-$	$[422]_{\frac{5}{2}}^+$	$\uparrow \uparrow$	this work
212.8	$1^+$	$[312]_{\frac{3}{2}}^-$	$[303]_{\frac{5}{2}}^-$	$\uparrow \downarrow$	[16]

<sup>a</sup> $\uparrow \uparrow$  means  $K = \Omega_p + \Omega_n$ ;  $\uparrow \downarrow$  means  $K = |\Omega_p - \Omega_n|$ .



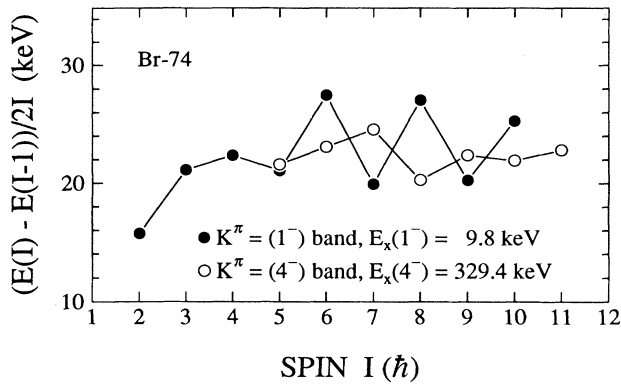


FIG. 6. Moment-of-inertia parameters  $\hbar^2/(2\Theta)$  for the bands built on the  $(1^-)$  and  $(4^-)$  states at 9.8 and 329.4 keV, respectively, as a function of the spin of the initial state.

Fig. 6. The smooth behavior at low spins changes to an alternating pattern above spin  $5\hbar$  expressing signature splitting. The kinematical moments of inertia  $J^{(1)}$  are shown in Fig. 7 versus the rotational frequency. Starting at large values at low spins the moments decrease to a relatively constant value of about  $22 \hbar^2 \text{MeV}^{-1}$ . Such values are typical in the mass region considered.

#### F. $K^\pi = (4^-)$ band built on the 329.4 keV level

The  $(4^-)$  state at 329.4 keV deexcites to several lower-lying states, but the most intense transition is a 128.6 keV  $\gamma$  ray to the  $(3^-)$  level at 200.8 keV. It also decays via a weak 256.6 keV  $E2$  transition to the  $(2^-)$  member of the  $K^\pi = (1^-)$  band. The higher-lying states of this band deexcite by in-band  $E2$  transitions and by  $M1$  transitions to members of the  $(1^-)$  band. This decay pattern leads us to suppose a similar internal parentage between both bands. Thus, the  $(4^-)$  state may originate from the same Nilsson configurations as suggested for the  $(1^-)$  band but with parallel coupling of the particle angular momentum components, which would be supported also by the GM rule. Therefore, the 2-qp configuration  $(\pi[312]_{3/2}^- \otimes \nu[422]_{5/2}^+)4^-$  is suggested for the state at 329.4 keV. For the sake of comparison the cas-

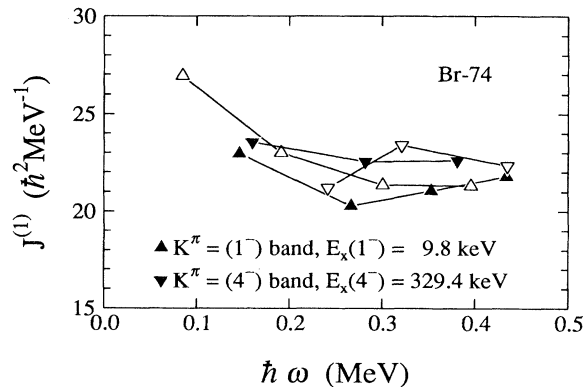


FIG. 7. Kinematical moments of inertia  $J^{(1)}$  for the bands built on the  $(1^-)$  and  $(4^-)$  states at 9.8 and 329.4 keV, respectively, as a function of rotational frequency. Full and open symbols are used for signatures  $\alpha = 0$  and  $\alpha = 1$ , respectively.

cade of  $\gamma$  rays feeding into the level at 329.4 keV has been analyzed in the same way as the  $(1^-)$  band. The moment-of-inertia parameters deduced are also shown in Fig. 6, and the kinematical moments of inertia  $J^{(1)}$  are given in Fig. 7 as a function of rotational frequency. The numbers obtained are very similar to the results of the  $(1^-)$  band. But the odd-even staggering of the moment-of-inertia parameters of the  $(4^-)$  band is smaller and of opposite phase compared to the  $(1^-)$  band. Possibly, this difference arises from level repulsion due to a residual interaction between levels of the same spin.

#### G. $K^\pi = (3^-)$ band built on the 85.9 keV level

The  $(3^-)$  state at 85.9 keV has previously been interpreted [16] as a bandhead state with the tentative configuration assignment of  $(\pi p_{3/2} \otimes \nu g_{9/2})$  based on the  $E1$  transition probabilities of the 72.1 and 188.4 keV  $\gamma$  rays. Later picosecond lifetime measurements [10] revealed large  $E2$  transition strengths for the  $\gamma$ -ray cascade built on top of it which implies a strongly deformed shape with an average value of  $\beta_2 = 0.34$ .

In our decay scheme several members of this  $(3^-)$  band are populated by some  $\Delta I = 0, 1$  transitions, e.g., at energies of 127.6, 243.8, 341.4, and 449.2 keV decaying from states of the  $(4^-)$  band on top of the 329.4 keV level. This might be a hint of similarities in their internal structures. Thus, we propose the 2-qp Nilsson configurations  $(\pi[310]_{1/2}^- \otimes \nu[422]_{5/2}^+)3^-$  as the main component for the bandhead state at 85.9 keV. Here the odd neutron moves in the same Nilsson orbital  $[422]_{5/2}^+$  as in the  $(4^-)$  band. The  $[310]_{1/2}^-$  Nilsson orbital arising from the  $f_{5/2}$  subshell is thought to be involved in the  $(\frac{1}{2}^-)$  state observed at 179.3 keV in  $^{75}\text{Br}$  [8]. Particle rotor calculations performed for the neighboring odd-proton nucleus  $^{73}\text{As}$  [40] predict also a low-lying  $\frac{1}{2}^-$  state arising from the  $[310]_{1/2}^-$  orbital which may correspond to the experimentally observed  $[\frac{1}{2}^-]$  state at 84.0 keV in  $^{73}\text{As}$ .

The proposed 2-qp configuration would harmonize with the GM rule which predicts a low-lying  $3^-$  state.

#### H. $K^\pi = (4^-)$ band built on the 238.7 keV level

The  $(4^-)$  level at 238.7 keV decays to the  $4^{(+)}$  isomer only. No other decay branch could be identified, from this state or even from the higher-lying members of the sequence built on it. A possible explanation for this situation might be an internal structure of this band that differs from those of the other negative-parity states.

So far, a  $(1^-)$  state at 89.6 keV has been interpreted [16] in terms of the 2-qp configuration  $(\pi[431]_{3/2}^+ \otimes \nu[303]_{5/2}^-)1^-$  where the unpaired proton moves in the  $g_{9/2}$  subshell. The GM rule suggests here that the intrinsic state with antiparallel coupling mode is energetically favored. The parallel coupling of these two Nilsson orbitals leads to a  $4^-$  configuration that might be the dominating component of the  $(4^-)$  state at 238.7 keV. In this case, the internal structure of this level sequence would be characterized by an unpaired proton in a  $g_{9/2}$  substate, while in most other negative-parity bands the

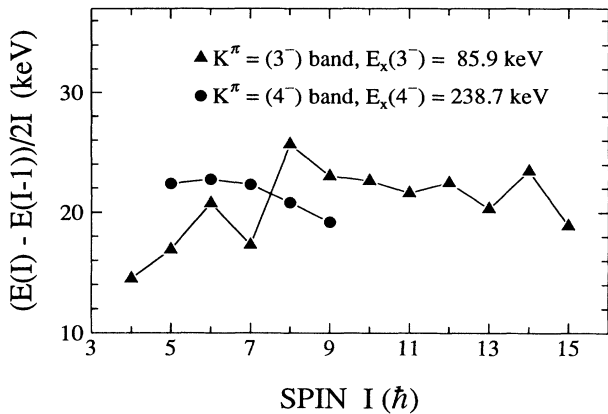


FIG. 8. Moment-of-inertia parameters for the bands on top of the  $(3^-)$  and  $(4^-)$  states at 85.9 and 238.7 keV, respectively, as a function of the spin of the initial state.

unpaired neutron occupies a  $g_{9/2}$  orbital. An additional hint to a different internal structure of the  $(4^-)$  state at 238.7 keV can be seen in the almost vanishing fluctuations of the moment-of-inertia parameters of this band which is in contrast to the data derived for the other bands (see Figs. 8 and 9).

### I. Other high-spin 2-qp states

In addition to the low-lying 2-qp states interpreted as heads of collective structures at prolate deformation, there are three more negative-parity states of high spin, e.g., the  $(5^-)$ ,  $(6^-)$ , and  $(7^-)$  states at 394.7, 485.8, and 990.1 keV excitation energy, respectively. All three states are connected in some way by  $\Delta I = 1, 2$  transitions to members of the  $(3^-)$  band, but they do not carry their own collective structure.

On the basis of prolate deformation of  $\beta_2 \approx 0.3$  the formation of 2-qp Nilsson states of at least spin  $5\hbar$  at low excitation energy is very unlikely. But they can easily be formed if a nonaxial or oblate deformation is assumed. For oblate deformation the high- $\Omega$  members of the  $g_{9/2}$  subshell are lowered in energy and can be occupied by a valence proton or neutron. The occurrence of triaxiality or oblate deformation at low excitation energies has recently been discussed in both the odd-proton nucleus  $^{73}\text{Br}$  [27, 33] and the odd-neutron nuclei  $^{73,75}\text{Se}$  [37, 42] and  $^{75}\text{Kr}$  [28].

### V. SUMMARY

The results of a study of high-spin states of  $^{74}\text{Br}$  with the  $^{58}\text{Ni}(^{19}\text{F}, 2pn)^{74}\text{Br}$  and  $^{65}\text{Cu}(^{12}\text{C}, 3n)^{74}\text{Br}$  reactions

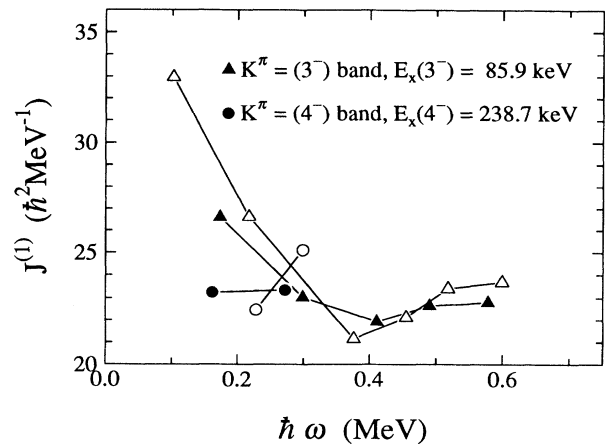


FIG. 9. Kinematical moments of inertia  $J^{(1)}$  for the bands on top of the  $(3^-)$  and  $(4^-)$  states at 85.9 and 238.7 keV, respectively, as a function of rotational frequency. Full and open symbols are used for signatures  $\alpha = 0$  and  $\alpha = 1$ , respectively.

have been presented. Several new states of medium spin, partly grouped into bands, have been found decaying to the ground state and/or to the  $4^{(+)}$  isomer. In this way the excitation energy of this isomer has been determined to be 13.8 keV and, thus, the energies of all states feeding into it are fixed. These new results make  $^{74}\text{Br}$  the best known odd-odd nucleus in the mass region  $A \sim 70-80$  and, thus, these data represent a significant challenge to theoretical model calculations. The low excitation energy of the isomer fits well into the previous picture that  $^{74}\text{Br}$  is strongly deformed and supports the assumption of positive parity for the isomer, which was shown to be consistent with the measured magnetic moment. In most cases 2-qp Nilsson configurations have been proposed for the observed bandheads.

*Note added in proof.* Very recently, a paper [43] has been published about magnetic moments and shape coexistence in the light Br isotopes, where an updated value for the magnetic moment of the  $4^{(+)}$  isomer in  $^{74}\text{Br}$ ,  $\mu = \pm 1.82(1)\mu_N$ , is given. This value has been interpreted on the basis of the 2-qp Nilsson configurations  $(\pi[431]_{3/2}^+ \otimes \nu[422]_{5/2}^+)4^+$  in agreement with our discussion.

### ACKNOWLEDGMENTS

This work was supported in part by the U.S. National Science Foundation. The authors would like to thank Prof. J.X. Saladin for his many contributions to the Pitt-FSU detector array. The help of J. Kerber from the FZ Rossendorf, Institut für Kern- und Hadronenphysik, in preparing the  $^{65}\text{Cu}$  target is acknowledged.

- [1] C.J. Lister, B.J. Varley, H.G. Price, and J.W. Olness, Phys. Rev. Lett. **49**, 308 (1982).  
 [2] S.L. Tabor, P.D. Cottle, J.W. Holcomb, T.D. Johnson, P.C. Womble, S.G. Buccino, and F.E. Durham, Phys. Rev. C **41**, 2658 (1990).

- [3] J. Heese, D.J. Blumenthal, A.A. Chishti, P. Chowdhury, B. Crowell, P.J. Ennis, C.J. Lister, and Ch. Winter, Phys. Rev. C **43**, R921 (1991).  
 [4] D.F. Winchell, M.S. Kaplan, J.X. Saladin, H. Takai, J.J. Kolata, and J. Dudek, Phys. Rev. C **40**, 2672 (1989).

- [5] M.A. Cardona, G. Garcia Bermúdez, A. Filevich, and E. Achterberg, *Phys. Rev. C* **42**, 591 (1990).
- [6] G. Winter, J. Döring, W.D. Fromm, L. Funke, P. Kemnitz, H. Prade, and E. Will, *Nucl. Phys.* **A367**, 95 (1981).
- [7] A.J. Kreiner, M.A.J. Mariscotti, C. Baktash, E. der Mateosian, and P. Thieberger, *Phys. Rev. C* **24**, 148 (1981).
- [8] L. Lühmann, M. Debray, K.P. Lieb, W. Nazarewicz, B. Wörmann, J. Eberth, and T. Heck, *Phys. Rev. C* **31**, 828 (1985).
- [9] W. Nazarewicz, J. Dudek, R. Bengtsson, T. Bengtsson, and I. Ragnarsson, *Nucl. Phys.* **A435**, 397 (1985).
- [10] J.W. Holcomb, T.D. Johnson, P.C. Womble, P.D. Cottle, S.L. Tabor, F.E. Durham, and S.G. Buccino, *Phys. Rev. C* **43**, 470 (1991).
- [11] S.G. Buccino, F.E. Durham, J.W. Holcomb, T.D. Johnson, P.D. Cottle, and S.L. Tabor, *Phys. Rev. C* **41**, 2056 (1990).
- [12] A.J. Kreiner and M.A.J. Mariscotti, *Phys. Rev. Lett.* **43**, 1150 (1979).
- [13] I. Hamamoto, *Phys. Lett. B* **235**, 221 (1990).
- [14] P.B. Semmes and I. Ragnarsson, *Proceedings of the International Conference on High Spin Physics and Gamma-Soft Nuclei, Pittsburgh, PA*, edited by J.X. Saladin, R.A. Sorensen, and C.M. Vincent (World Scientific, Singapore, 1991), p. 500.
- [15] G. Garcia Bermúdez, A. Filevich, A.J. Kreiner, M.A.J. Mariscotti, C. Baktash, E. der Mateosian, and P. Thieberger, *Phys. Rev. C* **23**, 2024 (1981).
- [16] G. Winter, J. Döring, W.D. Fromm, L. Funke, P. Kemnitz, and E. Will, *Z. Phys. A* **309**, 243 (1983).
- [17] W. Neumann, L. Cleemann, J. Eberth, T. Heck, G.S. Li, M. Nolte, and J. Roth, in *Proceedings of the Conference on High Angular Momentum Properties of Nuclei, Oak Ridge, Tennessee, 1982*, edited by N.R. Johnson (Oak Ridge National Laboratory, 1982), Vol. 1, p. 66.
- [18] A. Coban, *J. Phys. A* **7**, 1705 (1974).
- [19] H. Schmeing, J.C. Hardy, R.L. Graham, and J.S. Geiger, *Nucl. Phys.* **A242**, 232 (1975).
- [20] C. Ekström and L. Robertsson, *Phys. Scr.* **22**, 344 (1980).
- [21] A. Coban, J.C. Lisle, G. Murray, and J.C. Willmott, *Part. Nucl.* **4**, 108 (1972).
- [22] D.H. Lueders, J.M. Daley, S.G. Buccino, F.E. Durham, C.E. Hollandsworth, W.P. Bucher, and H.D. Jones, *Phys. Rev. C* **11**, 1470 (1975).
- [23] J. Döring, J.W. Holcomb, T.D. Johnson, S.L. Tabor, P.C. Womble, and G. Winter, Contributions to the International Conference on Nuclear Structure at High Angular Momentum, Ohawa, 1992, Chalk River Report No. AECL 10613, 1992 (unpublished), p. A13.
- [24] S.L. Tabor, M.A. Riley, J. Döring, P.D. Cottle, R. Books, T. Glasmacher, J.W. Holcomb, J. Hutchins, G.D. Johns, T.D. Johnson, T. Petters, O. Tekyi-Mensah, P.C. Womble, L. Wright, and J.X. Saladin, *Proceedings of the International Conference on Application of Accelerators in Research and Industry*, Denton, Texas, 1992 [Nucl. Instrum. Methods (to be published)].
- [25] J. Döring, G. Winter, L. Funke, P. Kemnitz, and E. Will, *Z. Phys. A* **305**, 365 (1982).
- [26] R. Zigelboim (private communication).
- [27] J. Heese, N. Martin, C.J. Gross, W. Fieber, K.P. Lieb, A. Kuhnert, K.H. Maier, and X. Sun, *Phys. Rev. C* **41**, 1553 (1990).
- [28] M.A. Herath-Banda, A.V. Ramayya, L. Cleemann, J. Eberth, J. Roth, T. Heck, N. Schmal, T. Mylaeus, W. Koenig, B. Martin, K. Bethge, and G.A. Leander, *J. Phys. G* **13**, 43 (1987).
- [29] T.D. Johnson, J.W. Holcomb, P.C. Womble, P.D. Cottle, S.L. Tabor, F.E. Durham, S.G. Buccino, and M. Matsuzaki, *Phys. Rev. C* **42**, 2418 (1990).
- [30] W.D. Schmidt-Ott, A.J. Hautojarvi, and U.J. Schrewe, *Z. Phys. A* **289**, 121 (1978); **295**, 341 (1980).
- [31] A.J. Kreiner, G. Garcia Bermúdez, M.A.J. Mariscotti, and P. Thieberger, *Phys. Lett.* **83B**, 31 (1981).
- [32] F. Pleiter, H. Bertschat, E. Recknagel, and B. Spellmeyer, *Nucl. Phys.* **A215**, 471 (1973).
- [33] N.J. Stone, C.J. Ashworth, I.S. Grant, A.G. Griffiths, S. Ohya, J. Rikovska, and P.M. Walker, in *Proceedings of the International Workshop on Nuclear Structure of the Zr Region, Bad Honnef, 1988*, edited by J. Eberth, R.A. Meyer, and K. Sistemich (Springer-Verlag, Berlin, 1988), p. 309.
- [34] P. Raghavan, *At. Data Nucl. Data Tables* **42**, 189 (1989).
- [35] J. Döring, G. Winter, L. Funke, B. Cederwall, F. Lidén, A. Johnson, A. Atac, J. Nyberg, G. Sletten, and M. Sugawara, *Phys. Rev. C* **46**, R2127 (1992).
- [36] C.J. Gallagher and S.A. Moszkowski, *Phys. Rev.* **111**, 1282 (1958).
- [37] F. Seiffert, R. Schwengner, G. Winter, L. Funke, W. Lieberz, R. Reinhardt, K.P. Schmittgen, D. Weil, R. Wrzal, K.O. Zell, and P. von Brentano, *Z. Phys. A* **340**, 141 (1991).
- [38] N.D. Newby, *Phys. Rev.* **125**, 2063 (1962).
- [39] P.C. Sood, R.K. Sheline, and R.S. Ray, *Phys. Rev. C* **35**, 1922 (1987).
- [40] B. Heits, H.-G. Friederichs, A. Rademacher, K.O. Zell, P. von Brentano, and C. Protop, *Phys. Rev. C* **15**, 1742 (1977).
- [41] B.O. Ten Brink, P. Van Nes, C. Hoetmer, and H. Verheul, *Nucl. Phys.* **A338**, 24 (1980).
- [42] T.D. Johnson, T. Glasmacher, J.W. Holcomb, P.C. Womble, S.L. Tabor, and W. Nazarewicz, *Phys. Rev. C* **46**, 516 (1992).
- [43] A.G. Griffiths, C.J. Ashworth, J. Rikovska, N.J. Stone, J.P. White, I.S. Grant, P.M. Walker, and W.B. Walters, *Phys. Rev. C* **46**, 2228 (1992).